Pergamon

SCIENCE DIRECT®

Bioorganic & Medicinal Chemistry 11 (2003) 4585–4589

BIOORGANIC & MEDICINAL CHEMISTRY

The 3D-QSAR Study of Antitumor Arylsulfonylimidazolidinone Derivatives by CoMFA and CoMSIA

Hea-Young Park Choo,[a,*] Suyoung Choi,[a] Sang-Hun Jung,[b] Hun Yeong Koh[c] and Ae Nim Pae[c,*]

[a]*School of Pharmacy, Ewha Womans University, Seoul 120-750, South Korea*
[b]*College of Pharmacy, Chung-Nam National University, Taejon 305-764, South Korea*
[c]*Biochemicals Research Center, Korea Institute of Science and Technology, PO Box 131, Cheongryang, Seoul 130-650, South Korea*

Received 20 March 2003; accepted 28 July 2003

Abstract—Three-dimensional quantitative structure–activity relationship (3D-QSAR) studies for a series of arylsulfonylimidazolidinone derivatives having antitumor activity were conducted using comparative molecular field analysis (CoMFA) and comparative molecular similarity indices anaysis (CoMSIA). The in vitro cytotoxicity against human lung carcinoma (A549) exhibited a strong correlation with steric and electrostatic factors of the molecules. Four different types of models have been built using CoMFA and CoMSIA method with AM1 charge or Gasteiger–Huckel charge. By comparison of the statistical results of these models, model I obtained by CoMFA study with AM1 showed the best predictability of the antitumor activities based on the cross-validated value (0.642), conventional r^2 (0.981), standard error of estimate (0.106) and PRESS value (0.170).

Introduction

Diarylsufonylureas have been investigated for the treatment of hard to cure non-hematogeneous cancers in the past decades.[1,2] Even though the mechanism of actions of these compounds has not been elucidated, it is estimated that diarylsulfonylureas act on mitochondria and are different from other clinically used antineoplastic agents in view of potency and toxicity.[3] Diarylsufonylureas show neither side effects exhibited by other anticancer agents, nor the cross-resistance in multidrug-resistant cell lines. Despite some of these merits, the development of diarylsulfonylurea has been seriously hampered due to the occurrence of the unexpected methemoglobinemia and anemia in phase II, which are caused by the aniline class metabolites. To avoid the production of the aniline class metabolite, Jung and coworkers have prepared arylsulfonylimidazolidinones containing sulfonylurea motif and evaluated their cytotoxicity.[4–14] Most of the analogues prepared showed much more potent activity against the various human cancer cell lines such as human lung carcinoma A549 and human melanoma SK-Mel-2 than sulofenur. The structural features essential for the activity of this series as follows; (1) small aromatic ring at the 4-position of imidazolidinone is necessary for the activity,[6] (2) the two phenyl groups should reside in certain distance, about 8.7 Å,[12] (3) introduction of bulky group at the 4-position of the phenyl group on sulfonyl function enhanced the activity,[13] and (4) near-planar conformation of the imidazolidinone ring is necessary, especially in the urea region.[15] Furthermore, the introduction of 1-substituted benzoylindoline as an aryl moiety of arylsulfonylimidazolidinones show increased activity.[16]

To understand the structural basis for the cytotoxic activity and to guide the design of more potent compounds, we analyzed the 3D-QSAR models on 4-phenyl - (*N* - substituted) - arylsulfonylimidazolidinones which have various substituents on nitrogen in indoline using CoMFA and CoMSIA.

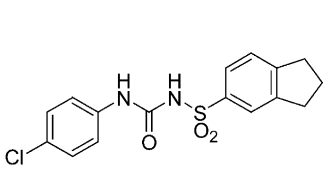

Sulofenur

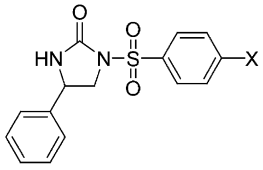

Arylsulfonylimidazolidinones

*Corresponding author. Tel.: +82-2-3277-3042; fax: +82-2-3277-2851; e-mail: hypark@mm.ewha.ac.kr

0968-0896/$ - see front matter © 2003 Elsevier Ltd. All rights reserved.
doi:10.1016/S0968-0896(03)00530-3

Methods

Data set for analyses

A set of the antitumor activity data on human lung carcinoma (A549) cell line of S-H Chung was used for this analysis.[16] The cytotoxicity was measured in vitro using sulforhodamine B (SRB) assay. Tables 1 and 3 represent the structures and antitumor activities (IC_{50}, μM) of compounds employed in this study.

Computational methods

All molecular modeling and statistical analyses were performed using SYBYL 6.9 molecular modeling software (Tripos Inc.) on Silicon Graphics Origin 300 (IRIX 6.5). The 2D structure of each compound was built using SYBYL Build program with the default SYBYL settings. The 2D structure was converted to a 3D structure using Concord 4.0 program. The structural energy minimization was performed using the SYBYL energy minimizer (Tripos Force Field) and AM1 semi-emperical quantum mechanical charge or Gasteiger–Huckel charge, with a 0.005 kcal/mol energy gradient convergence criterion.

Low energy conformation was searched from extended conformation of X-ray crystal structure of (*S*)-(+)-1-[1-(4-aminobenzoyl)indoline-5-sulfonyl]-4-phenyl-4,5-dihydroimidazol-2-one.[15]

Calculation of CoMFA descriptors

Conventional CoMFA was performed with the QSAR option of SYBYL. The steric and electrostatic field energies were calculated using sp^3 carbon probe atoms with +1 charge. Maximum energy cutoff for steric and electrostatic energies was 30 kcal/mol. The CoMFA grid spacing was 2.0 Å in all three dimensions within the defined region. The partial least squares (PLS) method was used for fitting the 3D structural features and their biological activities. The optimum number of components in the final PLS model was determined by the q^2 value, obtained from the leave-one-out cross-validation technique.

Calculation of CoMSIA descriptors

The CoMSIA of the QSAR module of SYBYL was used for the analysis. Similarity indices between a compound and a probe atom were calculated. The common probe atom with charge +1, radius 1 Å, and hydrophobicity +1 was placed at the intersections of a regularly spaced lattice. The attenuation factor (α) was set at 0.3. To determine the similarity, the mutual distance between probe atom and the atoms of the molecules in the data set was considered. In this study, physicochemical properties such as the steric and electrostatic feature, and the hydrogen bond acceptor were considered. Including the hydrophobic feature and the hydrogen bond donor as a descriptor decreases statistical values. The equation reported by Malinowski was used to calculate the similarity indices.[17]

Molecular alignment

Using compound **3** as a template molecule, superposition of all sulfonylimidazolidinone derivatives was performed with common benzodihydropyrrolylsulfonyl-4-phenylimidazolidinone group in all compounds, as shown in Figure 1.

Table 1. Structure of 4-phenyl-1-*N*-arylsulfonylimidazolidines

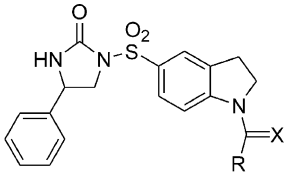

Compd	X	R
1[a]	O	$-NHCH_2CH_3$
2	O	$-NHCH(CH_3)_2$
3	O	$-NHC_6H_{11}$
4	O	$-NHC_6H_5$
5	O	$-NHC_6H_4(4\text{-}NH_2)$
6	S	$-NHCH_2CH_3$
7	S	$-NHCH_2CH_2CH_3$
8	S	$-NHCH_2CH_2CH_2CH_3$
9	S	$-NHC_6H_5$
10	O	$-NHC_6H_4$ (2-OCH_3)
11	O	$-NHC_6H_4$ (4-CH_3)
12	O	$-C_6H_5$
13	O	$-C_6H_4$ (2-OH)
14	O	$-C_6H_4$ (4-OEt)
15	O	$-C_6H_4$ (4-Cl)
16	O	$-C_6H_4$ (4-NO_2)
17	O	$-C_6H_4$ (4-CN)
18	O	$-C_6H_4$ (4-NH_2)
19	O	$-C_6H_4$ (3-Cl)
20	O	$-C_6H_4$ (3-F)
21	O	$-C_6H_3$ (2,4-F)
22	O	$-C_6H_4$ (3-OCF_3)
23	O	$-C_6H_4$ (4-OCF_3)
24[b]	O	$-NHCH_2CH_2CH_3$
25	O	$-NHC_6H_4$ (4-OCH_3)
26	S	$-NHCH_3$
27	S	$-NHC_6H_4$ (4-OCH_3)
28	O	$-C_6H_4$ (4-OCH_3)
29	O	$-C_6H_3$ (3,4-OCH_3)
30	O	$-C_6H_4$ (4-F)
31	O	$-C_6H_3$ (3,5-Cl)
32	O	$-C_6H_4$ (3-CF_3)

[a]Training set **1**–**23**.
[b]Test set **24**–**32**.

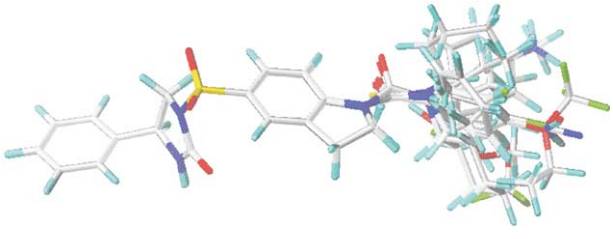

Figure 1. Stereoview of the **23** compounds superimposed.

Results and Discussion

The statistical results of the CoMFA and CoMSIA analyses using four different models of training set composed of 23 compounds are summarized in Table 2. In model I, semi-emperical AM1 charge was used. The CoMFA and molecular refractivity (CMR) were used as descriptors, and the antineoplastic activities (pIC_{50}) against human lung carcinoma (A549) as a dependent column. A cross-validated value q^2 which was obtained as a result of PLS analysis served as a quantitative measure of the predictability of the CoMFA model. Good cross-validated q^2 (0.642) and conventional r^2 (0.981) values proved the correlation between the descriptors and each of their activities, and gave reliability to the prediction of the antitumor activities of the test set. The relative contributions of steric and electrostatic field were 50.1 and 45.0%, respectively, and that of CMR was 0.5%. The contribution of steric fields was similar to electrostatic fields, but molecular refractivity gave a minor effect. The lipophilicity of the compounds (logP) did not enhance the correlation to activity and was excluded from QSAR analysis. The measured and estimated activities of the training set are reported with 0.054 of average value of the residuals in Table 3. The predictive residual sum of squares (PRESS) of the training set is 0.170, indicating good predictive model. The graph shows good linear correlation between estimated and measured values in Figure 2.

Table 2. QSAR results by using CoMFA and CoMSIA

Method	Model I CoMFA	Model II CoMSIA	Model III CoMFA	Model IV CoMSIA
Charge	AM1	AM1	Gasteiger–Huckel	Gasteiger–Huckel
ONC[a]	7	8	10	7
q^{2}[b]	0.642	0.510	0.246	0.493
r^{2}[c]	0.981	0.970	0.996	0.970
SEE[d]	0.106	0.137	0.055	0.133
F[e]	109.745	56.894	294.792	68.773
SF[f]	0.501	0.294	0.528	0.273
EF[g]	0.450	0.393	0.472	0.515
CMR[h]	0.050	—	—	
HA[i]	—	0.313	—	0.211
PRESS[j]	0.170	0.263	0.267	0.034
residual[k]	0.054	0.077	0.089	0.031
residual[l]	0.451	0.474	0.623	0.577

[a]Optimum number of component.
[b]Cross-validated r^2.
[c]Non-cross-validated r^2.
[d]Standard error estimate.
[e]Fraction of explained versus unexplained variance.
[f]Steric field.
[g]Electrostatic field.
[h]Calculated molecular refractivity.
[i]Hydrogen bond acceptor.
[j]Predictive residual sum of squares of the training set.
[k]Average residual of traning set.
[l]Average residual of test set.

Table 3. Measured and estimated activities of 23 compounds in the training set using model I

Compd	Measured IC_{50}[a]	Measured pIC_{50}[b]	Estimated[c]	Residual[d]
1	0.767	0.115	0.107	−0.008
2	0.170	0.769	0.770	0.001
3	0.006	2.194	2.254	0.060
4	0.385	0.415	0.347	−0.068
5	0.599	0.223	0.207	−0.016
6	1.017	−0.007	0.013	0.021
7	0.551	0.259	0.299	0.040
8	1.273	−0.105	−0.090	0.015
9	0.199	0.702	0.664	−0.038
10	0.274	0.562	0.537	−0.025
11	0.653	0.185	0.198	0.013
12	0.438	0.359	0.048	−0.311
13	1.376	−0.139	−0.113	0.026
14	0.205	0.687	0.613	−0.074
15	1.606	−0.206	−0.062	0.143
16	3.450	−0.538	−0.624	−0.086
17	3.365	−0.527	−0.491	0.036
18	0.195	0.711	0.737	0.026
19	3.361	−0.527	−0.387	0.140
20	0.705	0.152	0.205	0.053
21	4.006	−0.603	−0.577	0.026
22	5.153	−0.712	−0.701	0.011
23	1.308	−0.116	−0.102	0.014
Average				0.054

[a]Experimentally measured activity values (IC_{50}, μM).
[b]Experimentally measured activity values ($pIC_{50} = -\log IC_{50}$).
[c]Theoretically estimated activity values (pIC_{50}).
[d]|Measured−Estimated|.

The major steric and electrostatic features of the 3D QSAR derived from CoMFA study were illustrated in Figures 3 and 4 as 3D transparent surfaces. Steric contours indicate the location of a sterically less bulky group that enhances antitumor activity in the yellow color in this series of compounds. The long alkyl chain in compound **8** may have caused the decrease in the activity. The steric bulkness of isopropyl, allyl or cyclohexyl moiety attached to the imide nitrogen shown in the green region enhanced the activity. Electrostatic contours indicate the location of the electropositive character on phenyl substituent in blue that enhances antitumor activity. The electronegative substituents of the phenyl group such as nitro, cyano, dichloro, trifluromethoxy groups decreased the activities and the electon donating amine and ethoxy group enhanced the activity shown in blue color. The red color on the region of imide showed the electronegative group with an enhanced activity. Most of the compounds **1**–**11**

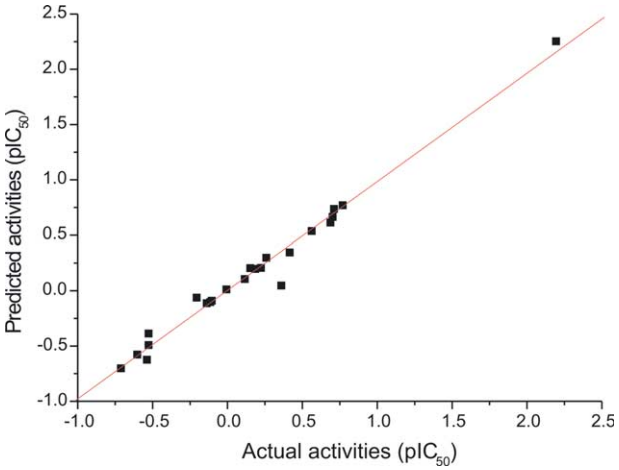

Figure 2. Measured versus estimated inhibitory activities of antitumor activities in model I.

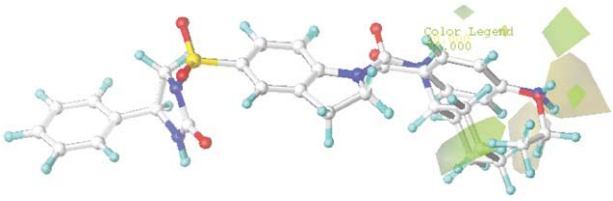

Figure 3. Steric field of CoMFA contour map in model I.

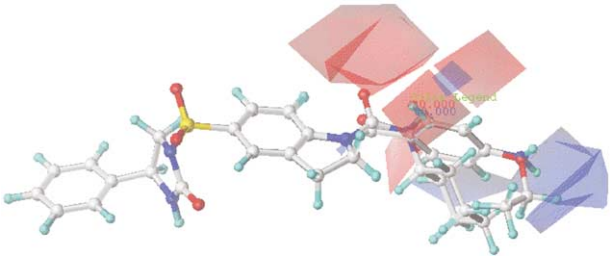

Figure 4. Electrostatic field of CoMFA contour map in model I.

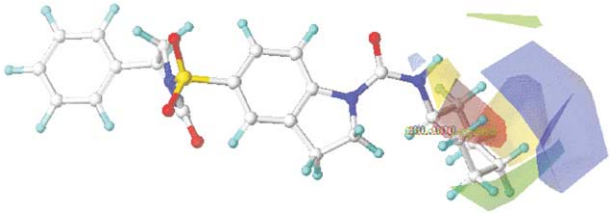

Figure 5. Steric and electrostatic field of CoMSIA contour map in model II.

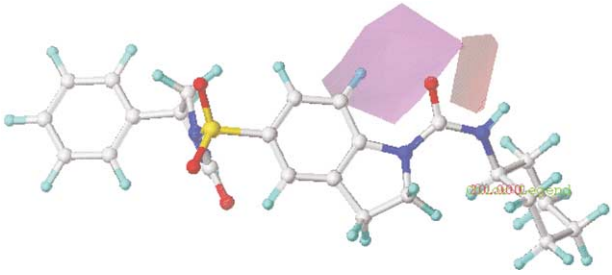

Figure 6. Hydrogen bond acceptor of CoMSIA contour map in model II.

possessing NH group showed better activity than the compounds **12**–**23**, having no NH group.

The CoMFA analysis of the test set composed of nine diarylsulfonyl derivatives was reported in Table 4. Most of compounds showed good agreement between actual and predicted values with 0.451 of average value of the residuals.

The CoMSIA studies with the same training set were performed. Steric, electrostatic and hydrogen bond acceptors were used as descriptors. The major steric, electrostatic features and hydrogen bond acceptor character of the 3D QSAR derived from CoMSIA study are illustrated in Figures 5 and 6 as 3D transparent surfaces. In this series, the statistical result of q^2, 0.510 and r^2, 0.970 obtained by CoMSIA model II was worse than the model I obtained by CoMFA, as shown in Table 2. However, we could expect that the hydrogen bond acceptor character was important at the position of thioimide or imide moiety using this model. By comparing with compounds **4** and **9** that are only different by an oxygen or sulfur atom, compound **9** showed better activity. Changing the several descriptors such as hydrogen bond donor, acceptor, hydrophobic and ClogP did not give any statistical improvement. In models III and IV, we tried Gasteiger–Huckel charge instead of AM1 charge on the CoMFA and CoMSIA study, which also did not provide increased results compared to model I. The statistical results are shown in Table 2. Among these QSAR models, we could use model I as a predictive model.

Table 4. Measured and estimated activities of nine compounds in the test set using model I

Compd	Measured IC_{50}[a]	Measured pIC_{50}[b]	Estimated[c]	Residual[d]
24	0.240	0.619	−0.053	−0.672
25	0.365	0.437	0.431	−0.006
26	0.221	0.656	1.158	0.502
27	2.495	−0.397	0.269	0.666
28	3.275	−0.515	0.292	0.807
29	3.255	−0.513	0.201	0.714
30	1.267	−0.103	−0.360	−0.257
31	3.919	−0.593	−0.187	0.406
32	4.237	−0.627	−0.659	−0.032
Average				0.451

[a]Experimentally measured activity values (IC_{50}, μM).
[b]Experimentally measured activity values (pIC_{50}).
[c]Theoretically estimated activity values (pIC_{50}).
[d]|Measured−Estimated|.

When arylsulfonylimidazolidinones were compared with sulofenur, they showed a superior antitumor activity. The antitumor activities (IC_{50}) of these compounds were 0.003–5 μg/mL, whereas sulofenur and doxorubicin showed 12.78 and 0.67 μg/mL, respectively.[16] That might be due to the electronegative nitrogen in indoline moiety and additional imide linkage on sulfonylimidazolidinone derivatives. Our 3D QSAR analysis indicates that a little bulky group but not a long chain on indoline moiety and the electropositive character of the substituents on phenyl moiety are important for the anticancer activity.

Conclusion

The 3D QSAR analyses of a set of diarylsulfonylureas with antitumor activity on human lung cancer cells (A529) were performed using CoMFA and CoMSIA. Based on the cross-validated value, standard error of estimate and average residuals, the CoMFA model I provided the most significant correlation of steric and electrostatic fields with the biological activities among the four models. According to this study, it can be concluded that the introduction of a little bulky and electron donating groups at indoline nitrogen would increase the activity.

Acknowledgements

This work was supported by a grant from Korea Research Foundation (01-B-WB-06-A-07).

References and Notes

1. Houghton, P. J.; Houghton, J. A. *Investig. New Drugs* **1996**, *14*, 271.
2. Howbert, J. J. *Drugs Future* **1991**, *16*, 517.
3. Ehjardt, W. J. *J. Drug Metab. Dispos.* **1991**, *19*, 370.
4. Jung, S. H.; Song, J. S.; Lee, H. S.; Choi, S. U.; Lee, C. O. *Bioorg. Med. Chem. Lett.* **1996**, *6*, 2553.
5. Jung, S. H.; Song, J. S.; Lee, H. S.; Choi, S. U.; Lee, C. O. *Arch. Pharm. Res.* **1996**, *19*, 570.
6. Jung, S. H.; Kwak, S. J. *Arch. Pharm. Res.* **1997**, *20*, 283.
7. Jung, S. H.; Lee, H. S.; Song, J. S.; Kim, W. M.; Han, S. B.; Lee, C. W.; Lee, M. S.; Choi, D. R.; Lee, J. A.; Chung, Y. H.; Yoon, S. J.; Moon, E. Y.; Hwang, H. S.; Seong, S. K.; Lee, D. K. *Bioorg. Med. Chem. Lett.* **1998**, *8*, 1547.
8. Moon, E. Y.; Choi, C. H.; Seong, S. K.; Lee, J.; Ryu, J. M.; Lee, M.; Jung, S. H.; Chung, Y. H.; Lee, D. K.; Yoon, S. J. *J. Appl. Pharmacol.* **1998**, *6*, 395.
9. Moon, E. Y.; Seong, S. K.; Jung, S. H.; Lee, M.; Lee, D. K.; Rhee, D. K.; Pyo, S.; Yoon, S. J. *Cancer Lett.* **1999**, *140*, 177.
10. Moon, E. Y.; Hwang, H. S.; Choi, C. H.; Jung, S. H.; Yoon, S. J. *Arch. Phar. Res.* **1999**, *22*, 565.
11. Hwang, H. S.; Moon, E. Y.; Seong, S. K.; Choi, C. H.; Chung, C. H.; Jung, S. H.; Yoon, S. J. *Anticancer. Res.* **1999**, *19*, 5087.
12. Jung, S. H.; Kwak, S. J.; Kim, N. D.; Lee, S. U.; Lee, C. O. *Arch. Phar. Res.* **2000**, *23*, 35.
13. Lee, H. S.; Park, K. L.; Choi, S. U.; Lee, C. O.; Jung, S. H. *Arch. Pharm. Res.* **2000**, *23*, 579.
14. Kim, I. W.; Jung, S. H. *Arch. Pharm. Res.* **2002**, *25*, 421.
15. Park, K. L.; Moon, B. G.; Jung, S. H.; Kim, J. G.; Suh, I. H. *Acta Crystal.* **2000**, *C56*, 1247.
16. Yoon, S. J.; Chung, Y. H.; Lee, M. S.; Choi, D. R.; Lee, J. A.; Lee, H. S.; Yun, H. R. Lee, D. K.; Moon, E. Y.; Hwang, H. S.; Choi, C. H.; Jung, S. H. WO 98/07719, PCT/KR 97/00154.
17. Klebe, G.; Abraham, U.; Mietzner, T. *J. Med. Chem.* **1994**, *37*, 4130.